RSC Sustainability

ROYAL SOCIETY OF CHEMISTRY

PAPER

View Article Online
View Journal | View Issue

Cite this: *RSC Sustainability*, 2025, **3**, 1909

Vortex fluidic-mediated transesterification enhancement of mongongo fatty acid ethyl ester production for haircare applications†

Xuejiao Cao,[a] Xuan Luo,[a] Safira M. Barros,[a] Wenjin Xing,[a] Melanie MacGregor,[a] Iliana Delcheva,[a] Jonathan A. Campbell,[a] Shan He,[ab] Bradley P. Kirk,[c] Youhong Tang[a] and Colin L. Raston[*a]

Fatty acid ethyl esters (FAEE) are one of the most popular ingredients in the organic cosmetic market due to their versatile functionality. However, its production technique aligning with the principle of green chemistry and adhering to organic standards remains unexplored. This study investigated the use of the vortex fluidic device (VFD), a versatile thin-film processing device that can generate substantial mechanical energy within a rapidly rotating tube, to assist in the sustainable and efficient production of Mongongo FAEE. Using the VFD, a FAEE yield of 92.65% was achieved within 20 minutes of processing, 1.3 times more effective than that attained *via* bench-top methods. Proton nuclear magnetic resonance (^{1}H NMR) and gas chromatography-mass spectrometry (GC-MS) confirmed the preservation and elevated concentrations of polyunsaturated FAEE following VFD processing. Furthermore, Mongongo FAEE was investigated for its application in hair protection. In a custom hair styling simulation experiment, a comparative analysis of Mongongo oil with FAEE demonstrated that Mongongo FAEE exhibited superior coverage efficiency on the hair surface, masking 95% of sulphur and nitrogen from the hair surface. This results in reduction in pore size, improved surface integrity, enhanced gloss, and minimised cysteine oxidation of hair. In the sun protection test, the FAEE-treated hair demonstrates a uniform morphology after 8 hours of sunlight exposure. Overall, it has been shown that a high yield of Mongongo FAEE was effectively achieved *via* VFD processing, while also demonstrating the ability to use the product in haircare applications.

Received 4th December 2024
Accepted 24th February 2025

DOI: 10.1039/d4su00763h

rsc.li/rscsus

Sustainability spotlight

This study introduces a sustainable approach to producing cosmetic-grade fatty acid ethyl esters (FAEE) from Mongongo oil using the vortex fluidic device (VFD). By eliminating hazardous solvents and minimising energy consumption, the method adheres to green chemistry principles while preserving FAEE properties. It supports UN Sustainable Development Goals 12 (Responsible Consumption and Production) and 3 (Good Health and Well-Being) by leveraging renewable plant-based resources and promoting environmentally friendly, skin-safe manufacturing practices. The resulting FAEE offers significant potential for eco-conscious applications in organic cosmetics, particularly in hair protection, addressing the industry's need for greener, safer alternatives. This work advances sustainable innovation in cosmetic manufacturing, contributing to a more responsible and health-conscious global industry.

1 Introduction

Organic cosmetics are formulated using natural-based ingredients, free from synthetic additives such as parabens, phthalates, sulphates, and hazardous solvents, which are often linked to skin sensitivity and environmental pollution.[1,2] A growing consumer preference for organic cosmetic products as safer alternatives to conventional formulations has been observed, driven by heightened awareness of the environmental and health risks posed by synthetic compounds.[1,2] To ensure sustainability, these ingredients are often derived from renewable natural resources.[3,4] The strictest standards for organic cosmetics COSMOS mandate that at least 95% of the ingredients must be of natural origin.[5] Additionally, the production process of bio-based ingredients must involve minimal chemical modification, simplified processing, and reduced environmental impact, aligning with key green chemistry principles such as waste prevention and safer chemical synthesis.[5] This

[a]*Flinders Institute for Nanoscale Science and Technology, College of Science and Engineering, Flinders University, Adelaide, 5042, Australia. E-mail: colin.raston@flinders.edu.au*

[b]*School of Food and Pharmacy, Zhejiang Ocean University, Zhejiang, 316022, China*

[c]*Institute for Photonic and Advanced Sensing, School of Physics, Chemistry and Earth Science, University of Adelaide, South Australia 5005, Australia*

† Electronic supplementary information (ESI) available. See DOI: https://doi.org/10.1039/d4su00763h

standard is consistent with the UN Sustainable Development Goals (SDGs), particularly SDG 12 (Responsible Consumption and Production) and SDG 3 (Good Health and Well-being).[6,7] The global market size for organic cosmetics reached US$ 48.4 billion in 2023, with a projected annual expansion rate of 5.1% over the subsequent decade.[8] This trend reflects rising consumer interest in healthier lifestyles and environmental sustainability.[2] Therefore, the cosmetic industry is consistently exploring sustainable and safe pathways for synthesis and production.[9]

One potential ingredient of choice in organic cosmetics is vegetable-based fatty acid ethyl esters (FAEE), demonstrating its versatility in applications such as biosurfactant, antioxidant, fragrance, flavour, and emollient function.[10] Plant-based FAEE offers better stability, and skin biocompatibility with better penetration efficiency.[11] In particular, FAEE with elevated polyunsaturated fatty acid content has been reported to exhibit cardioprotective, antiatherogenic, anti-inflammatory, and UV-protection properties.[12–14] Mongongo oil, also known as Manketti oil, originates from the nuts of the *Schinziophyton rautanenii* trees in Zambia, South Africa. It distinguished itself from other oils by its high levels of α-eleostearic acid, a unique conjugated fatty acid with suppressive effects on tumour growth,[15] is used for cellular repair.[16,17] Mongongo oil is also a cost-effective material in the cosmetic area, containing unsaturated fatty acids (UFAs), including linoleic and oleic, and is a potential candidate for various cosmetic products with hydrating, anti-inflammatory, tissue-regenerating, and restructuring properties.[10] Considering the aforementioned benefits, Mongongo oil-based FAEE has great potential in organic cosmetics. While numerous studies have utilised unsaturated vegetable oils such as sunflower and soybean oils as raw materials to get plant-based FAEE,[18–20] there is limited research exploring the cosmetic applications of FAEE derived from Mongongo oil.

The production of FAEE for the cosmetic industry is derived from transesterification reactions using renewable plant oils.[21,22] Traditional transesterification using benchtop method requires organic solvent which also involves prolonged processing, high-temperature and pH adjustment.[23] From a cosmetic industry viewpoint, these traditional processing methods might compromise unsaturated carbon bonds in polyunsaturated fatty acids (PUFA), which are pivotal for bioactivities.[24] The presence of organic solvent residues such as hexane and chloroform post-traditional processing also poses human health risks. Additionally, the extended processing duration and the requirement for heat introduce considerable time and energy demands, significantly driving up manufacturing costs.[23] Alternative methods have been investigated, including the use of biocatalysts, such as enzymes, to produce FAEEs under ambient conditions, but utilising enzymes such as lipases for transesterification, which can be costly and need specially designed immobilised biolipids systems.[25,26] The process also requires low temperatures, restricting its widespread adoption in industry.[27] As such, there is a need to establish a transesterification protocol for bio-based FAEE production in the cosmetic industry that is both environmentally sustainable and cost-effective.

One potential method for sustainable production of FAEEs is through the use of the vortex fluidic device (VFD). The VFD, illustrated in Fig. 1, serves as a versatile thin-film processing platform with diverse applications in both research and industry.[28–30] VFD technology applies intense micro-mixing to achieve high mass and heat transfer which overcome the mixing limitations inherent to conventional batch processing.[31,32] The operation of VFD relies on a rapidly rotating tube, which generates a thin film of liquid whose thickness is controlled by the rotational speed and tilt angle of the tube, and the sample volume.[33] Two distinct types of topological fluid flows within the liquid thin film are generated in the VFD, both down to submicron dimensions.[31,34] These are spinning top or typhoon-like flow and double helical flow influenced by the Faraday wave eddies affected by the Coriolis force.[35] These fluid flows are the driving forces initiating chemical reactions and increasing the product yield.[32,36] The VFD has also been employed for nanocarbon processing including the one-step assembling of C_{60} molecules into

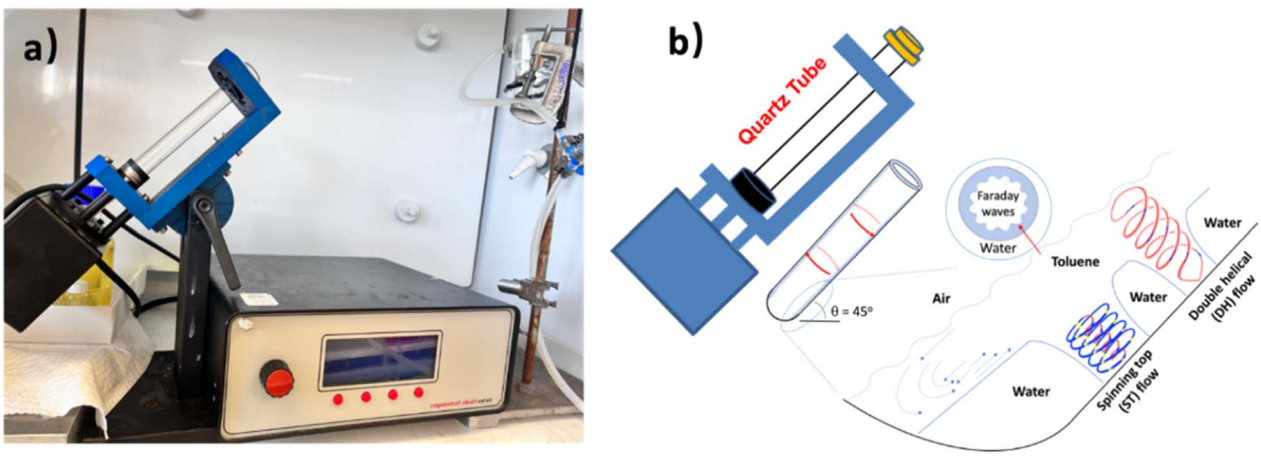

Fig. 1 The introduction of VFD. (a) Photograph of the VFD. (b) Schematic of a VFD (confined mode) operation and the high shear topological fluid flows in the rotating tube.

nanotubes, rods, cones, and spicules in the absence of surfactant.[34,37] Furthermore, the application of VFD extends to small-molecule synthesis, material processing for drug delivery and hydrogel production.[32,38,39] While the applications of the vortex fluidic device (VFD) in food science, medical science, and chemistry have been widely explored through green processes, its application in producing sustainable ingredients for organic cosmetics industries remains largely unexplored.

This study aims to produce cosmetic-grade Mongongo oil-based fatty acid ethyl esters (Mongongo FAEE) using the VFD, with a focus on green chemistry, environmental sustainability, and enhanced bioactivity. The VFD method employs a hazardous solvent-free approach, and efficient production process, and preserves the structural integrity of the FAEE products, aligning with green chemistry principles and the Sustainable Development Goals, particularly SDG 12 (Responsible Consumption and Production) and SDG 3 (Good Health and Well-being). The resulting FAEE is assessed for its potential in haircare applications, specifically for protecting hair from heat styling (160 °C for 5 minutes) and prolonged natural sunlight exposure (35 °C, 8 hours).

2 Materials and method

2.1 Materials

Chloroform, D-chloroform, ethanol, sodium hydroxide (NaOH) and phenolphthalein indicator, were analytical grade and purchased from Sigma-Aldrich. Shampoo, Mongongo oil and virgin hair were provided by Plantworx company (Adelaide, Australia).

2.2 FAEE production

The FAEE was produced by micro-mixing oil and NaOH–ethanol (1.5% w/v) solution with the ratio of 1 : 3 (v/v) using the VFD at the speed of 7750 rpm for 20 minutes, and traditional benchtop methods (water bath) were operated as the control experiment. These parameters, including rotational speed, catalyst concentration, and the NaOH-to-ethanol-to-oil ratio, were studied and optimised in a previous study using response surface methodology.[40] VFD processing uses the mechanical energy generated by the rotating tubes to produce FAEE at room temperature, in contrast to the traditional benchtop method that relies on applying heat. The standard VFD was equipped with a quartz tube of 20 mm external diameter, positioned at a tilt angle (θ) of 45° relative to the horizontal position. This specific tilt angle was determined as the optimal operating parameter for efficient shearing. After 20 minutes of reaction, the mixture was placed in an ice box for 20 minutes to stop the reaction. After washing with distilled water, the top layer (FAEE layer) was collected and dried at 40 °C for 2 hours. The yield of the Mongongo FAEE is evaluated by the equation below:

$$\text{Mongongo FAEE yield}(\%) = \frac{\text{the mass of Mongongo FAEE(g)}}{\text{the mass of Mongongo oil(g)}} \times 100 \quad (1)$$

The FAEE produced by traditional procedure was referred to the reported methods with minor modifications.[41] The condition of catalyst concentration (1.5% w/v), oil–ethanol ratio (1 : 3 v/v) and reaction time (20 min) remained the same in this control experiment. The traditional process of FAEE requires 70 °C and constantly stirring conditions. After 20 minutes of reaction, the mixture was placed in an ice box for another 20 minutes to halt the reaction and facilitate a comparison of the efficiency between the two methods.

2.3 Mongongo oil and FAEE characterisations

2.3.1 Fourier transform infrared spectroscopy (FTIR). Attenuated total reflectance (ATR) was performed in combination with infrared spectrometry using a FTIR for sample testing. All the samples were scanned over the range 500–4000 cm^{-1} with 16 scans and a resolution of 4 cm^{-1}.

2.3.2 Gas chromatography-mass spectrometry (GC-MS). GC-MS analysis was performed on a Varian CP-3800 gas chromatography unit coupled with a 2200 Saturn MS detection unit. The injection temperature was set at 40 °C, increasing at a rate of 20 °C per minute until reaching 300 °C. A reverse-phase column (30 M × 25 mM × 0.25 mM) was employed, and the mass spectrometry data were analysed using NIST 05 molecular recognition software. Each sample (0.01 mL) was mixed with 1 mL chloroform for GC-MS analysis. The percentage of each Mongongo FAEE in the composition was determined based on the corresponding peak area obtained from the GC-MS results.

2.3.3 Nuclear magnetic resonance (^{1}H NMR). ^{1}H NMR spectra of FAEE were acquired using a 600 MHz Bruker spectrometer. Standard quantitative parameters, such as a delayed pulse (D1) of 10.00 and 16 scans, were employed to assess the sample. A drop of sample was diluted with 0.5 mL of deuterated chloroform for testing.

2.3.4 Contact angle analysis. For the contact angle analysis, a goniometer model OCA25 (DataPhysics Instrument, Germany) was used. Images of droplets with volume of about 2 μL were collected. Multiple locations on the substrate – commercially available hydrophobic adhesive film, fixed on a microscope glass slide – were probed. The images of the droplet profiles were processed with the equipment software (SCA20, version 6.1.11) to measure the static contact angles of Milli-Q water, Mongongo oil and Mongongo FAEE on the hydrophobic surface.

2.4 Mongongo FAEE application on haircare

2.4.1 Hairstyling process. The virgin hair was evenly treated with 0.5 mL Mongongo oil/FAEE by soft brush and then straightened at 160 °C with a home-use thermal iron. The morphology, flyaway property, pore size, reflection, and surface structure of hair were tested and compared.

2.4.2 Hair sun exposure test. The hair samples were fixed by glue on a glass Petri dish. A small volume (0.5 mL oil) and FAEE were applied to the hair surface by brushing it separately. The original hair, oil-treated hair, and FAEE-treated hair were exposed to sunlight for 8 hours in Adelaide (34° 55′ 16.4280″ S, 138° 35′ 58.2108″ E). The average exposed temperature was 35 °C, and the highest temperature was 38 °C. The sun-processed

samples were imaged by SEM to investigate their morphology before and after shampoo washing. The tensile machine and FTIR were used to study the change in hair structure.

2.4.3 Scanning electron microscopy (SEM). Samples were examined using a SEM at 5.0 kV, and a spot size of 4.0 nm, at 10 mm of working distance. Dried hair samples were directly fixed on conductive carbon adhesive tape, while a 2 nm thick layer of platinum was then sputtered on top of it before SEM analysis to avoid charging. The high-resolution images of the sample morphology were then acquired. The energy-dispersive X-ray (EDX) spectra from this region were also collected to determine the elemental composition and distribution (C, N, O, and S).

2.4.4 Microscope test of hair gloss. Images of samples were recorded using a Zeiss Axio Imager M2 Optical Microscope. The darkfield illumination was used to test the reflection of hair samples. The 5× magnification objective was used to take photos. The eyepiece was set at 50%, the darkfield reflection was 50%, and the light from the bottom of the microscope was 0 so that all the light captured was the reflection from hair samples. The image was processed by ImageJ.[42]

2.4.5 Tensile test. Tensile tests were performed to evaluate the mechanical behaviour of hair. The hair was washed by shampoo and dried at room temperature before testing. Each sample was prepared by cutting the middle section from a long hair strand, away from the hair root and tip. Only a single strand was mounted with grips and tested on a universal mechanical testing platform (Instron 5960) with a load cell capacity of 500 N. The load rate was set to 20 mm min^{-1}. The gauge length of each strand was 40 mm, and the diameter was measured around 40 μm with an optical technique. The mechanical platform automatically recorded the applied force and displacement.

2.4.6 Flyaway test. The hair with different treatments was rubbed for 10 s and the flyaway degrees were recorded by photo, and then processed by ImageJ.[42] The hair was washed with shampoo and dried at room temperature before testing.

2.4.7 Differential scanning calorimetry (DSC). The DSC technique was employed to examine the thermal characteristics of hair subjected to various drying conditions. The hair was washed with shampoo and dried at room temperature for DSC testing. 8 mg of each hair sample was analysed using a DSC instrument (DSC 8000, PerkinElmer). The samples underwent a thermal ramp from 25 °C to 300 °C at a heating rate of 10 °C min^{-1}, all under an inert nitrogen atmosphere.

2.4.8 Brunauer–Emmett–Teller (BET). The surface porosity of the hairs was assessed using the BET analytical method with a TriStar II instrument from Micrometric Ltd (Lincoln LN6 3RX, United Kingdom). The hair was washed by shampoo and dried at room temperature for BET testing. Before analysis, the hairs with different treatments were first crushed into a powder using liquid nitrogen. Subsequently, 40 mg of each powdered sample was placed at the base of a BET tube, which was then subjected to a 24 hours evacuation process at 100 °C to remove moisture. Following the evacuation, the tube was introduced into a BET analyser, operating under the following conditions: adsorptive gas N_2, bath temperature set at 77 K, and equilibration intervals of 20 s.

3 Results and discussion

3.1 Mongongo oil and its FAEE characterisation

Mongongo oil, characterised by significantly high degrees of unsaturation, has characteristic peaks at 992 cm^{-1} and 966 cm^{-1} in FTIR,[43] as shown in Fig. 2a. These peaks correspond to the CH vibrations in conjugated cis, trans, and *trans*-carbon–carbon bonds of α-eleostearic acid[10,17] of Mongongo oil. The ^1H NMR results shown in Fig. 2b–d illustrate the structure differences of Mongongo oil, FAEE produced in VFD, and FAEE from the benchtop method. Oils manifest two peaks between 4.1-4.3 ppm, originating from the triglyceride structure where hydrogen atoms of the external glycerol backbone are situated within the 4.1 to 4.3 ppm range,[44] denoted as peaks "a" and "c" in Fig. 2b. The peaks between 5 to 7 ppm, corresponding to the triple conjugate carbon–carbon double bond of α-eleostearic acid,[10] are represented as numbers 9, 11, and 13 in its fatty acid chain. In our study, the arising single quartet pattern in the products at 4.15 ppm labelled "a'" in Fig. 2c and d attributed to the CH_2 group in the ethyl esters, confirming the occurrence of the transesterification reaction. In addition, signals around 4.3 ppm labelled "c residues" in Fig. 2d indicate the remaining traces of mono-, di-, and triglycerides of FAEE produced by the traditional method, suggesting an incomplete progression of transesterification.[44] The absence of that peak in Fig. 2c indicated the full conversion of Mongongo FAEE from oil. Previous studies have attempted varied hourly durations to achieve chemical equilibrium in the transesterification reaction.[19,27] In this study, the 20 minutes traditional heating process proved insufficient for complete FAEE conversion from Mongongo oil, whereas the VFD efficiently achieved full conversion and favourable chemical equilibrium at room temperature. This efficiency is attributed to the unique high shear regimes of the VFD: at high rotational speeds, the liquid is rapidly distributed along the inner wall of the tube, forming a dynamic thin liquid film. Within this film, triglycerides and catalysts undergo rapid, uniform, and thorough micromixing, enabling fast and efficient transesterification. In the comparison of Mongongo FAEE composition between the VFD process and the traditional process, GC-MS results were analysed and shown in Fig. 2e–g. The VFD products exhibited nearly 50% higher peak intensity compared to those obtained through the conventional method, indicating an elevated FAEE concentration. Notably, the relative intensity of peak 5 in the VFD products was significantly higher than in the control, suggesting effective protection of the corresponding FAEE species. An additional advantage of VFD processing is the absence of solid formation, as shown in Fig. S1,† which is caused by saponification during transesterification processing.[45] This not only potentially improves the overall FAEE concentration but also simplifies the sample collection and container cleaning process.

The Mongongo oil fatty acid composition was reported to have 73% UFAs, close to 83% among the 5 main FAEE in this study. Ethyl α-eleostearic, reported to be 23.8% of Mongongo oil, showed a comparable proportion of 22.8% in our study. This FFA, containing triple conjugate C=C, is prone to damage

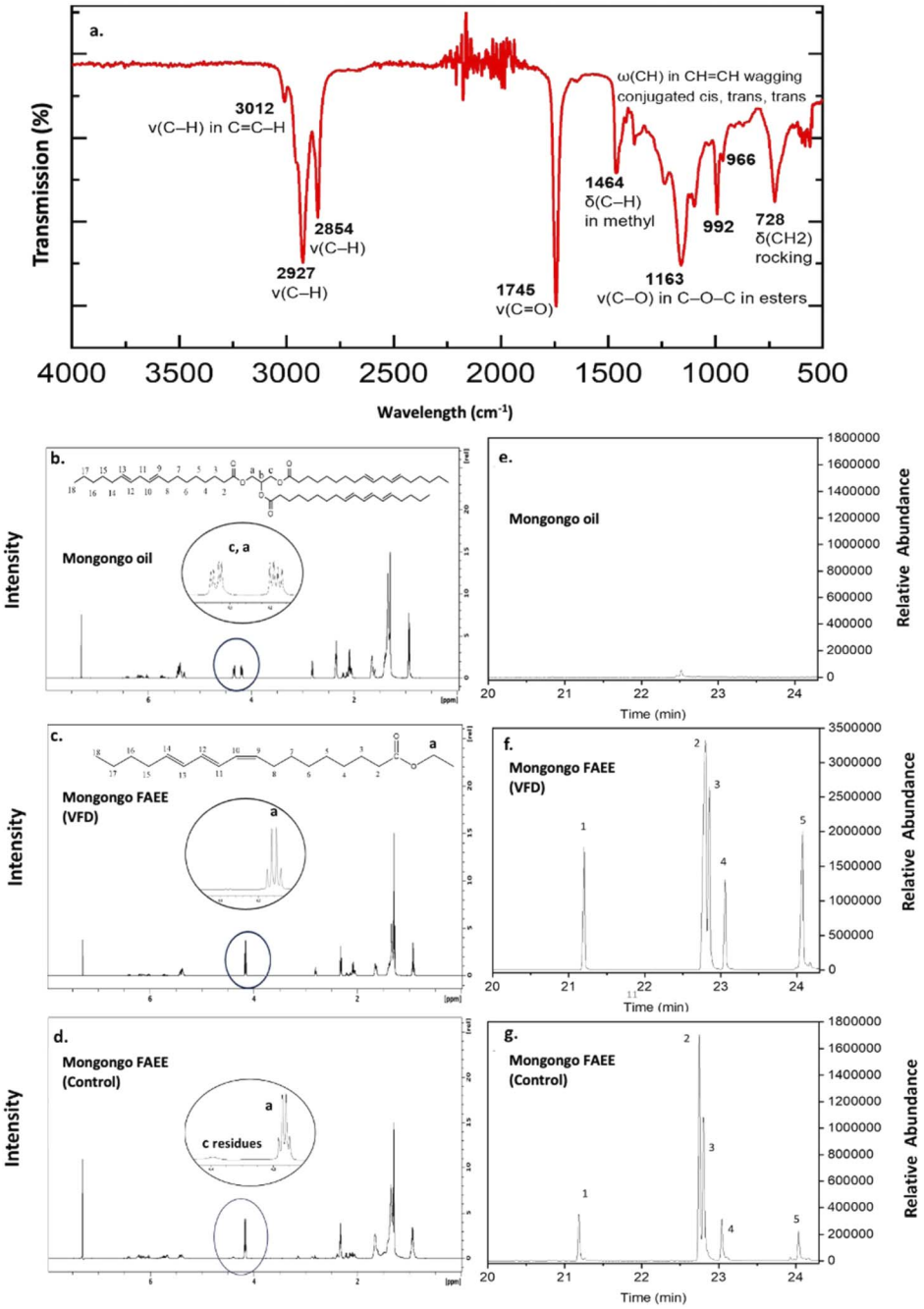

Fig. 2 The characterisation of Mongongo oil and Mongongo FAEE. VFD processing: confined mode, 7750 rpm, 20 min, room temperature. Control processing: water bath, 20 min, 70 °C. (a): FTIR spectra of Mongongo oil; (b)–(d): ^{1}H NMR spectra of Mongongo oil and Mongongo FAEE from VFD processing and control method; (e)–(g): GC-MS spectra of Mongongo oil and Mongongo FAEE from VFD and control method.

and increased by 16% during VFD processing, resulting in a relatively lower ratio of other saturated FAEE. This outcome can be attributed to the benign conditions of the VFD process, which involves no heating and consequently avoids damage to unsaturated FAEE during transesterification. It is evident that VFD processing significantly enhances FAEE production with an improvement in yield of about 20% as shown in Fig. 3. As previously mentioned, saponification reactions play a crucial role in influencing the equilibrium towards transesterification,[46] and heating conditions can cause the oxidation of C=C and damage polyunsaturated fatty acids,[47] resulting in lower production and unsaturation degree of FAEE. However, the conversion yield of FAEE from different plant oils varies, with high viscosity and acid value typically contributing to lower yields. The VFD consistently preserves the structure of unsaturated FAEE from various oils due to its room-temperature processing.

Another benefit of VFD technology is its scalability, as demonstrated in biofilm production.[48] The standard VFD used in this study requires minimal material, reducing energy and

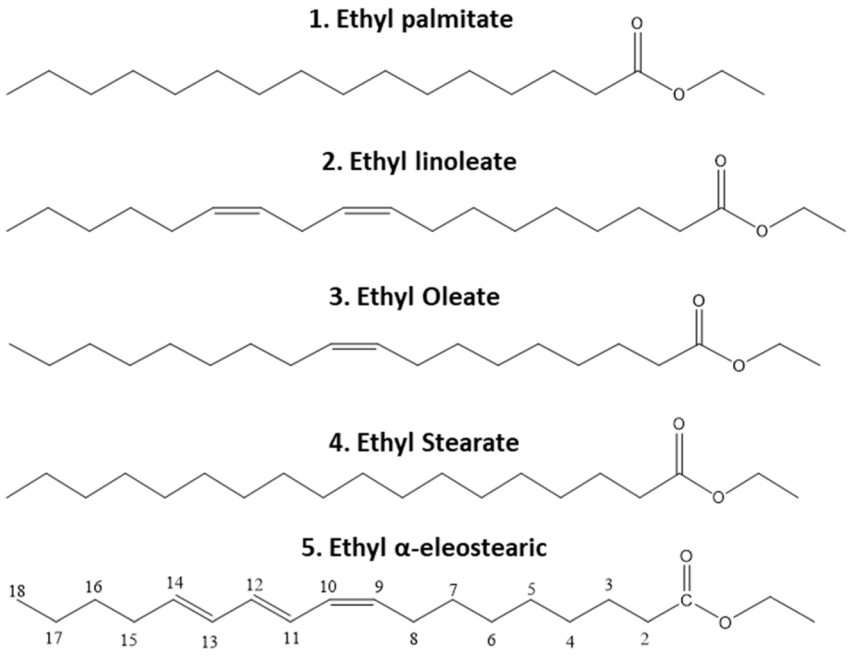

Peak	Resident Time (min)	Main FAEE	Mongongo FAEE VFD (%)	Mongongo FAEE Control (%)
1	21.18	Ethyl palmitate (C18:0)	8.49	8.82
2	22.75	Ethyl linoleate (C20:2)	39.7	22.75
3	22.80	Ethyl Oleate (C20:1)	20.48	34.39
4	23.05	Ethyl Stearate (C20:0)	7.80	8.08
5	24.18	Ethyl α-eleostearic (C20:3)	22.82	6.29
	Total Conversion Ratio		92.65	73.22

Fig. 3 The composition and yield of Mongongo FAEE from the VFD and control method. VFD processing: confined mode, 7750 rpm, 20 min, room temperature. Control processing: water bath, 20 min, 70 °C. 1–5 represent 5 peaks of FAEE shown in GC-MS spectra.

resource consumption and aligning with sustainability goals. Here, we focused on producing Mongongo FAEE and evaluating their efficiency for hair protection. While the current VFD design supports scalability, its capacity and adaptability can be further improved for industrial FAEE production.

The wetting properties of oil products have a significant influence on the contact and absorbance efficiency of skin and hair. Healthy human hair usually exhibits hydrophobic wetting properties.[49] The static contact angle of water on the surface probed in this study is 87°, which showcases the hydrophobic properties of the substrate, as shown in Fig. 4. The contact angle of FAEE is 37°, 31% lower in comparison to the Mongongo oil. The higher affinity of FAEE towards the solid surface is likely due to its simpler structure and shorter chain length, compared with the triglyceride structure of Mongongo oil. The Mongongo FAEE with a lighter texture and lower viscosity could spread

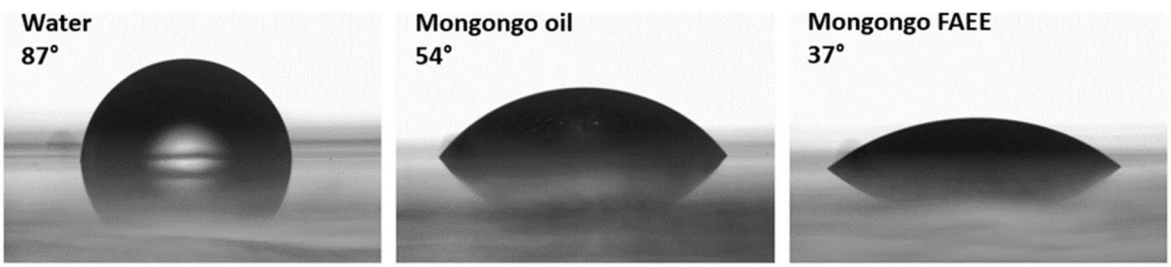

Fig. 4 Static contact angles of Mongongo oil and its FAEE on a hydrophobic surface.

faster and wider on the hydrophobic surface, which is expected to be beneficial in skin/hair contact and should provide a less greasing feeling.

3.2 Mongongo FAEE for hair protection during styling

3.2.1 Mongongo FAEE-treated hair morphology changes after hair styling. The hair shaft is characterised by three essential components: the outermost layer known as the cuticle, the centrally located cortex, and the innermost medulla.[43] The outermost cuticle structure influences the appearance, lustra, and surface structural integrity of hair.[50,51] The original hair displays a distinct scaly surface structure, whereas hair subjected to thermal iron treatment directly shows a cracked, diminished, and irregularly layered structure. This alteration is attributed to the partial damage of hair cuticles in direct contact with heat, leading to moisture loss and ultimately causing the hair to become dry and brittle.[52] In this study, we conducted a comparative analysis of the micromorphology of hair treated with Mongongo oil and Mongongo FAEE following thermal iron heating. Both oil and FAEE applications were observed to form a layer on the hair surface, differing from the original hair structure. Notably, the hair treated with FAEE displayed a smoother surface, while the oil-treated hair exhibited a rougher texture with partially exposed cuticles in Fig. 5.

Previous research has indicated that various hair treatments, such as bleaching, perming, and dyeing, inflict significant damage to hair, generating numerous microscale pores.[53] To assess the impact of Mongongo oil and Mongongo FAEE on hair integrity, we examined the pore size of hair by BET, as shown in Fig. 5. Since the hair was thoroughly washed with shampoo, the oil/FAEE does not influence the pore size. Thus, the measurement reflects the natural pore size of the hair, rather than pores filled with oil/FAEE. Both Mongongo oil and FAEE treatments demonstrated a noteworthy reduction in pore size and surface area, compared with hair heated by thermal iron directly. This finding aligns well with SEM results, revealing that untreated hair exhibited more surface defects and openings after hair styling, allowing greater penetration of nitrogen into the hair shaft. Conversely, hair treated with Mongongo oil and FAEE demonstrated a certain degree of preservation in hair surface integrity. Specifically, the BJH absorption cumulative surface area of pores, which typically represents pore volume, was determined for hair treated with FAEE, yielding a value of only 0.003 $m^2 g^{-1}$. This value corresponds to 60% of the surface area observed in oil-treated hair, further underscoring the efficacy of FAEE in maintaining hair surface integrity. This is also consistent with the DSC results in Fig. S2,† where FAEE-treated hair required a higher temperature (82.3 °C) to remove bound water. This suggests that hair with higher integrity retains moisture within the hair shaft more effectively, indicating that FAEE helps maintain the structural cohesion of the hair, reducing water loss. Elkady, *et al.*[54] reported that peaks at 235 °C and 246 °C correspond to the denaturation of keratin (ordered alpha-helices) and the complete thermal breakdown of the cystine, respectively. However, in our study, there was no significant difference in the temperature at which the peak a signals the onset of structural protein denaturation, nor the peak b indicating the final breakdown of the keratin network. This is reasonable, as thermal treatments like flat ironing, when applied within a reasonable time frame, do not significantly

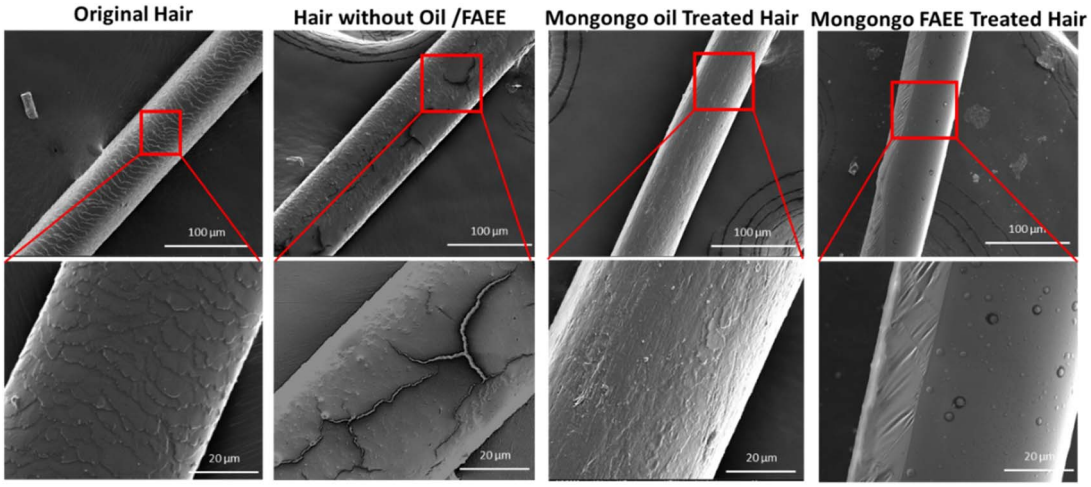

BET Data	BJH Adsorption cumulative volume of pores(cm^3/g)	BJH Adsorption cumulative surface area of pores (m^2/g)	Adsorption average pore width (Å)	Single point surface area (m^2/g)
Hair without Oil /FAEE	0.000110	0.113	39.076	0.0834
Mongongo Oil Treated Hair	0.000013	0.005	34.824	0.0131
Mongongo FAEE Treated Hair	0.000021	0.003	32.001	0.0152

Fig. 5 The SEM and BET of hair treated with Mongongo FAEE after hair styling. The hair was washed with shampoo before BET testing.

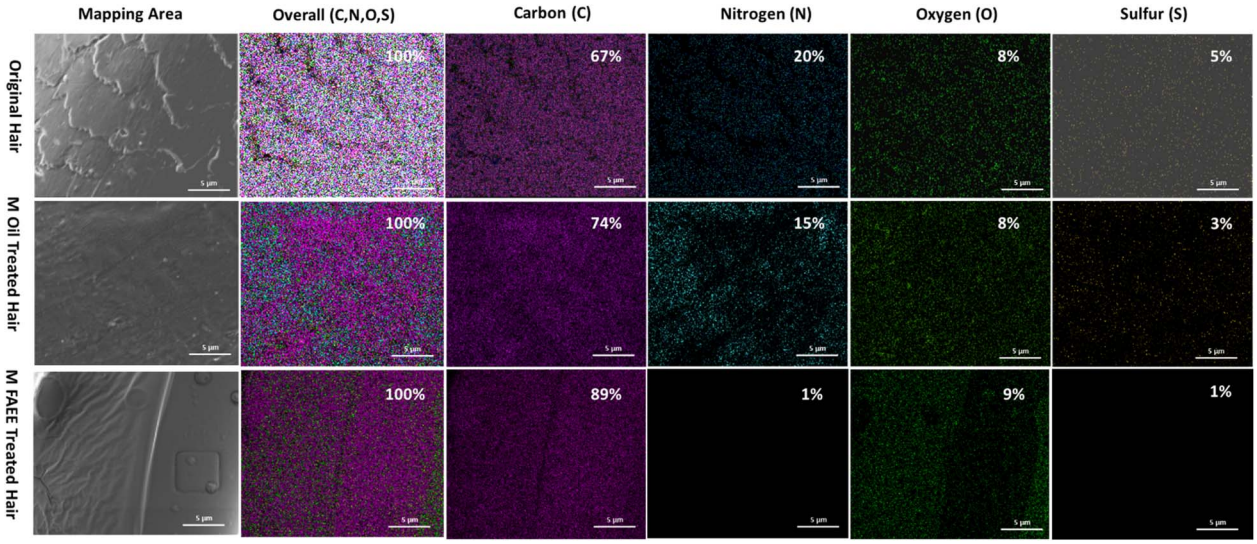

Fig. 6 The SEM-EDX of element analysis of hair treated with Mongongo FAEE after hair styling.

alter the dense cortex matrix in the innermost of the hair shaft. Consequently, no notable changes were observed in the denaturation temperature of keratin. This differs from the SEM, BET, and DSC water peak results, as the cuticle, located on the hair's surface, is more vulnerable to direct heat contact, leading to changes in morphology, surface porosity, and water retention capacity.

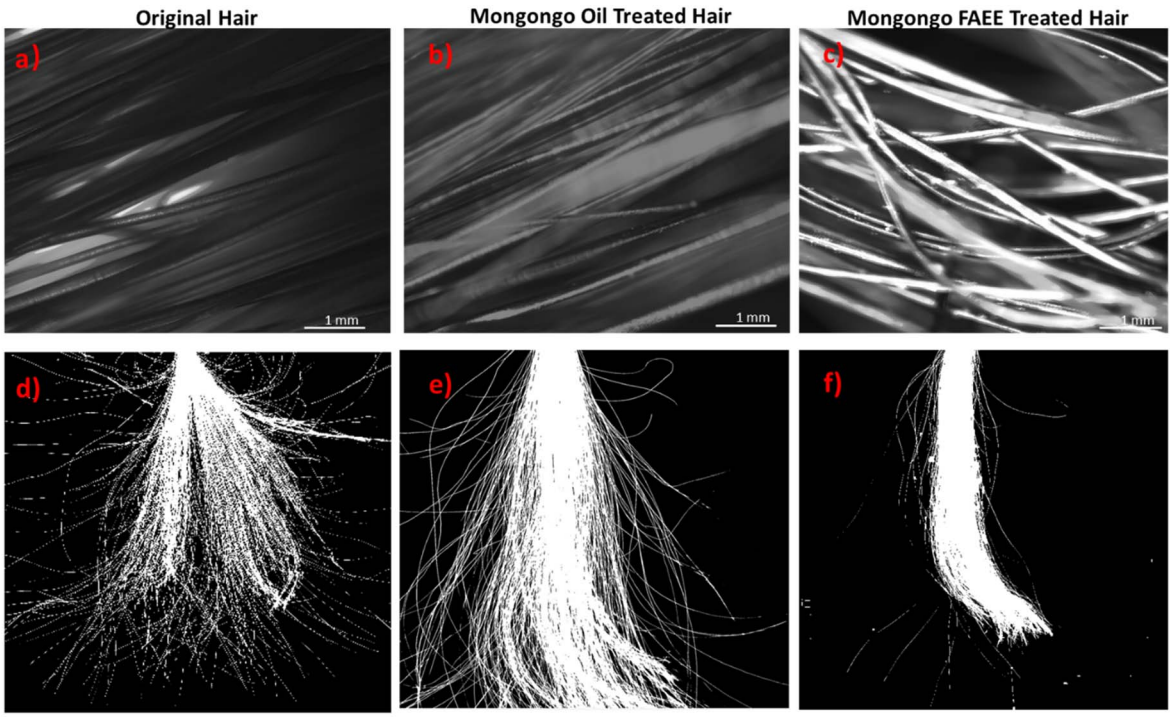

Pixel intensity (Image J)	Area	Mean	Min	Max	Integrated Density	Flyaway percentage
Original Hair	304315	44.45	16	255	13525290	75%
Mongongo Oil Treated Hair	306535	68.62	23	136	21034894	40%
Mongongo FAEE Treated Hair	283972	112.11	12	255	31836776	10%

Fig. 7 The gloss/flyaway improvement of hair treated with Mongongo FAEE. (a)–(c), gloss results; (d)–(f), flyaway results.

3.2.2 Mongongo FAEE coating efficiency in hair after hair styling. To ascertain the distinctions in hair morphology resulting from film coating rather than structural damage, SEM-EDX analysis was employed to further examine the composition of the hair surface (Fig. 6). Human hair, a form of keratin,[55] primarily consists of carbon (C), hydrogen (H), oxygen (O), nitrogen (N), and sulphur (S). In contrast, oil and FAEE exhibit compositions limited to C, H, and O. Lower levels of N and S on the hair surface indicate more efficient coverage by the coating material. For original hair, the elemental composition is as follows: carbon (C, 67%), nitrogen (N, 20%), oxygen (O, 8%), and sulphur (S, 5%). This composition is consistent with the presence of protein in the hair.[56] In the case of oil-treated hair, the distribution of C, H, O, N, and S is non-uniform. The surrounding location of the image displays higher levels of N and S, while the central region exhibits significantly lower levels (indicated by less blue and yellow). This suggests uneven coating, with the oil aggregating in specific areas rather than forming a uniform layer over the entire hair surface. Conversely, FAEE-coated hair exhibits almost absences of N and S, indicating close to 100% coverage on the hair surface. It may also benefit from its good fluidity and spread-ability on hydrophobic surfaces shown in the contact angle test. Fig. S3 in the ESI† provides a more detailed representation of the intensity of each element in different hair samples, illustrating coating efficiency and overall distribution of C, O, N and S.

3.2.3 Mongongo FAEE in gloss improvement after hair styling. Following hair styling, the applied heat induces moisture loss and results in brittleness, consequently impacting both the gloss and flyaway properties of the hair.[57] Our investigation involved a comparative analysis of hair gloss properties and brittleness levels, as shown in Fig. 7. Hair treated with FAEE after styling exhibited a markedly superior gloss degree,[49,58] nearly three times that of the original hair and twice that of Mongongo oil-treated hair according to pixel intensity results. This observation aligns with the inherent superior reflective ratio of FAEE, a characteristic that has historically contributed to enhancing hair shine properties.[59] Furthermore, the FAEE employed in our study demonstrated enhanced fluidity, facilitating superior coverage on the hair surface. As corroborated by SEM images, the smoother surface of FAEE-treated hair is directly linked to a significantly increased gloss, while the partial oil coating causes uneven light reflection on the hair surface. Additionally, following flyaway testing, FAEE-treated hair exhibited improved static properties, likely attributed to its heightened affinity to the hydrophobic surface of the hair. This discernible affinity underscores the advantageous impact of FAEE on minimising static-related issues.

3.2.4 Mongongo FAEE in thermal oxidation protection after hair styling. Cystine is a crucial dipeptide within the structural composition of hair,[60] as depicted in Fig. 8. Its sulphur (S) compounds play a vital role in cross-linking adjacent peptides, thereby preserving the integrity of the hair. Nevertheless, exposure to factors such as sunlight, air pollution, frequent hair washing, and styling practices can induce oxidative modifications to its structure, as indicated by prior studies.[61–63] Depending on the extent of damage, cystine may transform into cystine monoxide, cystine dioxide, and cysteic acid. This transformation usually results in a shift of hair from a highly hydrophobic surface to a hydrophilic one.[53] Notably, oxidative events induce alterations in specific peaks within FTIR spectroscopy, particularly those associated with sulphur-related structures. The peaks at 1175 cm^{-1} and 1044 cm^{-1} are documented due to the formation of S=O or O=S=O bonds.[64] Fig. 8b shows that the regions corresponding to amides A, B, I, II, and III exhibit minimal changes following simulated hair styling processes. It has been reported that the intensity of peaks at 1041 cm^{-1} and 1180 cm^{-1} increased following chemical treatment, indicating the conversion of cystine into cystine monoxide, cystine dioxide, cysteic acid, and sulfonates during the process.[65] While there was no significant difference in the peak intensity at 1041 cm^{-1}, a notable increase in peak intensity around 1175 cm^{-1} (circled) was observed in hair treated with Mongongo oil. In contrast, hair treated with FAEE showed

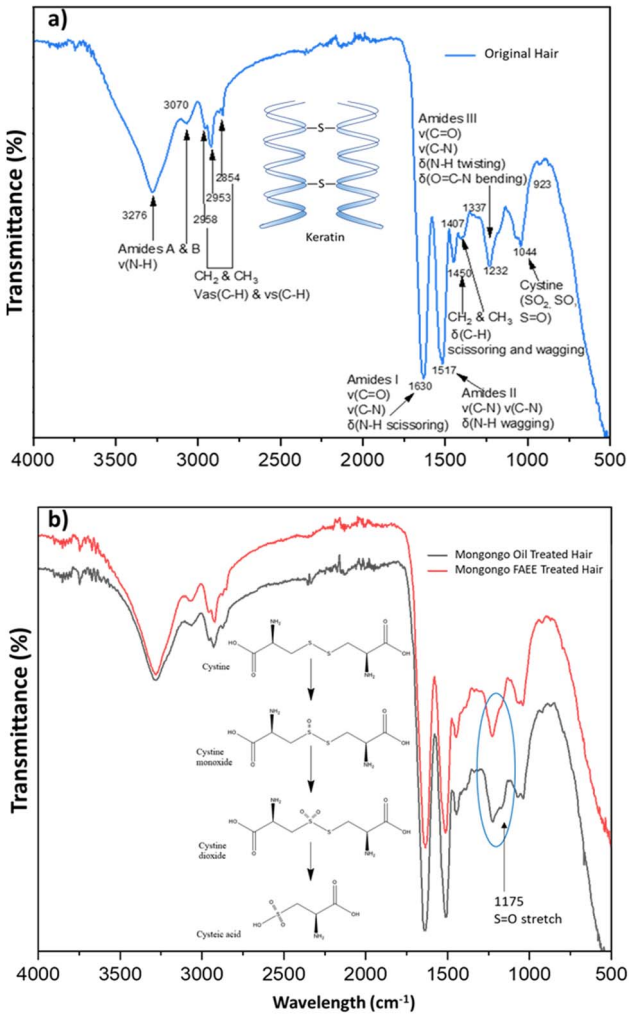

Fig. 8 FTIR spectra of hair treated with Mongongo FAEE after hair styling. All the hair was washed before testing. (a) FTIR spectra of original hair. (b) FTIR spectra of Mongongo oil-treated hair and Mongongo FAEE-treated hair.

a markedly lower peak intensity, suggesting less cystine oxidation. Considering the capability to probe surface structures of FTIR,[66] it can be inferred that FAEE provides enhanced protection against thermal oxidation on the hair surface. This finding aligns with the previous discussion, indicating that FAEE effectively distributes across the hair surface, shielding it from direct heat exposure during processing. Consequently, this protection contributes to the preservation of gloss and surface integrity.

3.2.5 Mongongo FAEE in thermal oxidation protection after hair styling. In the hair sun exposure test, it was anticipated that the stability and superior fluidity of FAEE would afford better hair protection against sunburn. Fig. 9 illustrates that Mongongo FAEE-treated hair maintains surface uniformity after 8 hours of sun exposure while Mongongo oil-treated hair exhibits uneven clumping. After shampoo washing, both oil-treated hair and FAEE-treated hair surfaces appear more uniform compared to untreated hair, where the cuticles remain open. Examining the overall picture of the hair sample in Fig. 9i, Mongongo oil forms a white aggregated solid on hair tress, while FAEE maintains stability without any undesirable appearance, as demonstrated in Video 1 in the ESI.† The FTIR spectra showed that the hair with Mongongo FAEE treated has a significantly lower intensity at 1150 cm^{-1} and 1044 cm^{-1} than that of oil-treated hair, indicating minimal cystine oxidation. However, despite the enhanced uniformity and less oxidation of the hair surface with FAEE treatment, there were no significant differences observed in the hair tensile test after 8 hours of

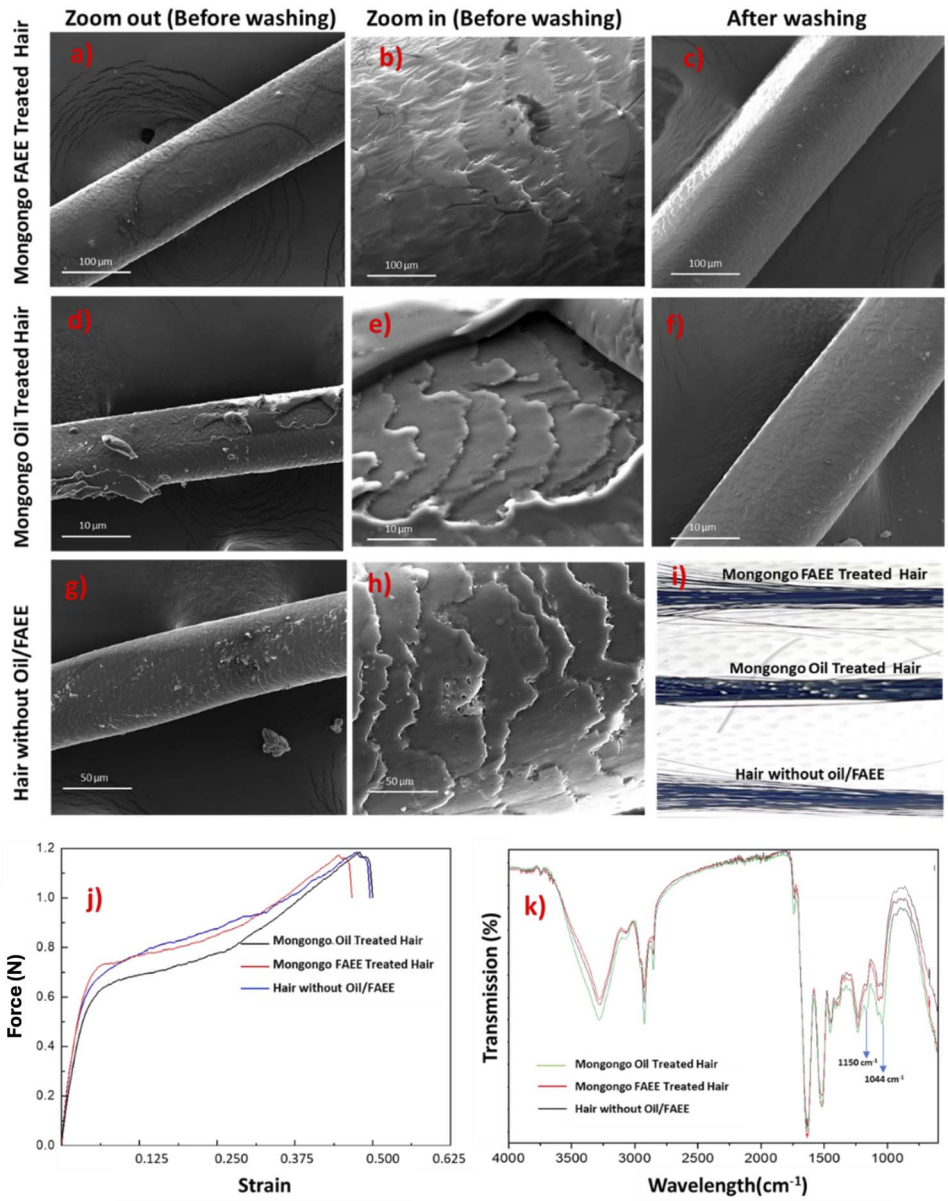

Fig. 9 Mongongo FAEE application in hair sun protection. (a)–(i) SEM, hair morphology changes after sun exposure. (j) the tensile test of hairs; (k) FTIR spectra of hair.

constant sunlight treatment. As shown in Fig. 9j, there was no apparent difference in the tensile responses between untreated and treated hair strands exhibiting almost identical levels of both yield force (~0.65 N) and peak force (~1.2 N). The unaltered tensile strength can be explained by the fact that the cortex, not the cuticle, is the major load-carrying component. Moreover, the surface defects in the form of pores and grooves are not deep enough so that they cannot readily propagate towards the centre under lower force, and thus have a negligible effect on the measured strength.[67] A study demonstrated that shampoos with different plant oils can enhance hair tensile strength.[68] Our future goals involve formulating the FAEE-based emulsion to facilitate penetration towards the hair shaft, aiming to enhance hair strength internally.

4 Conclusion

In our study, we successfully produced Mongongo FAEE from Mongongo oil using the VFD operating at room temperature within a 20 minutes timeframe. The yield of FAEE was notably high at 92% using the VFD, representing a significant 20% improvement compared to the traditional heating method. The Mongongo FAEE obtained through VFD processing demonstrated a superior unsaturation, maintaining its featured structure and ensuring a higher quality product for cosmetic application. The VFD process, utilising induced mechanical energy and requiring only ethanol, sodium hydroxide, Mongongo oil, and distilled water for FAEE production, exemplifies a green, environmentally friendly, and sustainable approach to efficient production. In simulated hair styling experiments, the Mongongo FAEE exhibited enhanced coverage efficiency on the hair surface after thermal iron treatment. The FAEE-treated hair displayed a smoother surface, increased surface integrity (smaller pore size in BET results), and superior gloss, aligning with aesthetic preferences. FTIR analysis of the hair surface revealed that FAEE treatment offered better protection. Besides, in simulated sun exposure tests, FAEE-treated hair not only exhibited improved surface structure but also demonstrated greater stability compared to Mongongo oil. Building upon the success of FAEE in hair applications, future scopes involve formulating FAEE-based emulsions to explore their penetration efficiency and internal effects on hair of strength and tensile properties.

Data availability

Data will be made available on request.

Author contributions

Xuejiao Cao: methodology, data collection, writing – original draft, visualisation. Xuan Luo: formal analysis, review and editing, validation. Safira M. Barros: methodology. Wenjin Xing: methodology, data interpretation. Melanie MacGregor: methodology, data interpretation, visualisation. Iliana Delcheva: methodology, data interpretation, visualisation. Jonathan Campbell: methodology, data interpretation. Shan He: formal analysis, visualisation. Bradley P. Kirk: formal analysis, validation. Youhong Tang: formal analysis, data interpretation, review and editing, supervision. Colin Raston: conceptualization, methodology, review and editing, supervision, project administration, resources, funding acquisition.

Conflicts of interest

The authors declare that they have no known competing financial interests or personal relationships that could have appeared to influence the work reported in this paper.

Acknowledgements

This research was made possible through the funding provided by ARC-ITTC for Green Chemistry in Manufacturing (IC190100034), Plantworx and ARC FT200100301. We are immensely grateful to Peter Francis and the Plantworx company for providing guidance and materials for the experiments.

References

1 Y. Y. Lin, T. Yang, L. Y. Shen, J. Zhang and L. P. Liu, Study on the properties of Dendrobiumofficinale fermentation broth as functional raw material of cosmetics, *J. Cosmet., Dermatol.*, 2022, **21**, 1216–1223, DOI: **10.1111/jocd.14197**.

2 R. S. Heath, R. E. Ruscoe and N. J. Turner, The beauty of biocatalysis: sustainable synthesis of ingredients in cosmetics, *Nat. Prod. Rep.*, 2022, **39**, 335–388, DOI: **10.1039/d1np00027f**.

3 J. Gubitosa, V. Rizzi, P. Fini and P. Cosma, Hair care cosmetics: From traditional shampoo to solid clay and herbal shampoo, a review, *Cosmetics*, 2019, **6**, 13, DOI: **10.3390/cosmetics6010013**.

4 H. Krohnert and M. Stucki, Life Cycle Assessment of a Plant-Based, Regionally Marketed Shampoo and Analysis of Refill Options, *Sustainability*, 2021, 13, DOI: **10.3390/su13158478**.

5 COSMOS, About the COSMOS-standard, *International Certification for Cosmetics*, 2023, **https://www.cosmos-standard.org/en/**.

6 D. M. Franks, J. Keenan and D. Hailu, Mineral security essential to achieving the Sustainable Development Goals, *Nat Sustainability*, 2023, **6**, 21–27, DOI: **10.1038/s41893-022-00967-9**.

7 R. A. Sheldon and D. Brady, Green chemistry, biocatalysis, and the chemical industry of the future, *ChemSusChem*, 2022, **15**, e202102628, DOI: **10.1002/cssc.202102628**.

8 G. V. Research, Organic Shampoo Market Size, Share & Trends Analysis Report By Distribution Channel (Supermarkets/Hypermarkets, Specialty Stores, Online), By Region, And Segment Forecasts, 2025–2030, 2024, **https://www.researchandmarkets.com/reports/6032589/organic-shampoo-market-size-share-and-trends?srsltid=AfmBOoqaHhz8LwnjgGQh0G6aGz9wg-bTMOKYpyI8-bpW102s4x9FIjZo**.

9 N. Amberg and C. Fogarassy, Green Consumer Behavior in the Cosmetics Market, *Resources*, 2019, **8**, 137, DOI: 10.3390/resources8030137.
10 N. Cheikhyoussef, M. Kandawa-Schulz, R. Böck and A. Cheikhyoussef, Mongongo/Manketti (Schinziophyton rautanenii) Oil, *Fruit Oils: Chemistry and Functionality*, 2019, pp. 627–640, DOI: 10.1007/978-3-030-12473-1_32.
11 M. Yi, *et al.*, Highly Valuable Fish Oil: Formation Process, Enrichment, Subsequent Utilization, and Storage of Eicosapentaenoic Acid Ethyl Esters, *Molecules*, 2023, **28**, 672, DOI: 10.3390/molecules28020672.
12 Q. Yao, T. Jia, W. Qiao, H. Gu and K. Kaku, Unsaturated fatty acid-enriched extract from Hippophae rhamnoides seed reduces skin dryness through up-regulating aquaporins 3 and hyaluronan synthetases 2 expressions, *J. Cosmet., Dermatol.*, 2021, **20**, 321–329, DOI: 10.1111/jocd.13482.
13 S. H. Park and H. K. Kim, Antibacterial activity of emulsions containing unsaturated fatty acid ergosterol esters synthesized by lipase-mediated transesterification, *Enzyme Microb. Technol.*, 2020, **139**, 109581, DOI: 10.1016/j.enzmictec.2020.109581.
14 M. Douguet, *et al.*, Spreading properties of cosmetic emollients: Use of synthetic skin surface to elucidate structural effect, *Colloids Surf., B*, 2017, **154**, 307–314, DOI: 10.1016/j.colsurfb.2017.03.028.
15 T. Tsuzuki, Y. Tokuyama, M. Igarashi and T. Miyazawa, Tumor growth suppression by α-eleostearic acid, a linolenic acid isomer with a conjugated triene system, via lipid peroxidation, *Carcinogenesis*, 2004, **25**, 1417–1425, DOI: 10.1093/carcin/bgh109.
16 N. Zimba, S. Wren and A. Stucki, Three major tree nut oils of southern central Africa: their uses and future as commercial base oils, *Int. J. Aromather.*, 2005, **15**, 177–182, DOI: 10.1016/j.ijat.2005.10.009.
17 N. Cheikhyoussef, *et al.*, Characterization of Schinziophyton rautanenii (Manketti) nut oil from Namibia rich in conjugated fatty acids and tocopherol, *J. Food Compos. Anal.*, 2018, **66**, 152–159, DOI: 10.1016/j.jfca.2017.12.015.
18 M. Elkelawy, *et al.*, Maximization of biodiesel production from sunflower and soybean oils and prediction of diesel engine performance and emission characteristics through response surface methodology, *Fuel*, 2020, **266**, 117072, DOI: 10.1016/j.fuel.2020.117072.
19 A. C. Lima, *et al.*, Evaluation and kinetic study of alkaline ionic liquid for biodiesel production through transesterification of sunflower oil, *Fuel*, 2022, **324**, 124586, DOI: 10.1016/j.fuel.2022.124586.
20 M. Udayakumar, Kinetics and thermodynamic analysis of transesterification of waste cooking sunflower oil using bentonite-supported sodium methoxide catalyst, *Biomass Convers. Biorefin.*, 2023, (13), 9701–9714, DOI: 10.1007/s13399-021-01836-9.
21 H. Hosseinzadeh-Bandbafha, *et al.*, Environmental life cycle assessment of biodiesel production from waste cooking oil: A systematic review, *Renewable Sustainable Energy Rev.*, 2022, **161**, 112411, DOI: 10.1016/j.rser.2022.112411.
22 V. S. Nagtode, *et al.*, Green Surfactants (Biosurfactants): A Petroleum-Free Substitute for Sustainability—Comparison, Applications, Market, and Future Prospects, *ACS Omega*, 2023, **8**, 11674–11699, DOI: 10.1021/acsomega.3c00591.
23 S. K. Bhatia, *et al.*, An overview on advancements in biobased transesterification methods for biodiesel production: Oil resources, extraction, biocatalysts, and process intensification technologies, *Fuel*, 2021, **285**, 119117, DOI: 10.1016/j.fuel.2020.119117.
24 S. C. H. Ndomou, *et al.*, Optimization of the mixture of groundnut, palm, stearin, and sesame oils subjected to heat treatment and evaluation of their lipid quality, *Heliyon*, 2023, e12813, DOI: 10.1016/j.heliyon.2023.e12813.
25 J. Aguilera-Oviedo, E. Yara-Varón, M. Torres, R. Canela-Garayoa and M. Balcells, Sustainable synthesis of omega-3 fatty acid ethyl esters from monkfish liver oil, *Catalysts*, 2021, **11**, 100, DOI: 10.3390/catal11010100.
26 A. Moschona, A. Spanou, I. V. Pavlidis, A. J. Karabelas and S. I. Patsios, Optimization of Enzymatic Transesterification of Acid Oil for Biodiesel Production Using a Low-Cost Lipase: The Effect of Transesterification Conditions and the Synergy of Lipases with Different Regioselectivity, *Appl. Biochem. Biotechnol.*, 2024, **196**, 8168–8189, DOI: 10.1007/s12010-024-04941-3.
27 A. Mustafa, *et al.*, Has the time finally come for green oleochemicals and biodiesel production using large-scale enzyme technologies? Current status and new developments, *Biotechnol. Adv.*, 2023, **69**, 108275, DOI: 10.1016/j.biotechadv.2023.108275.
28 S. He, N. Joseph, X. Luo and C. L. Raston, Vortex fluidic mediated food processing, *PLoS One*, 2019, **14**, e0216816, DOI: 10.1371/journal.pone.0216816.
29 J. Britton, S. B. Dalziel and C. L. Raston, The synthesis of di-carboxylate esters using continuous flow vortex fluidics, *Green Chem.*, 2016, **18**, 2193–2200.
30 X. Cao, *et al.*, Stability and Cleansing Function Enhancement of Organic Shampoo by a Vortex Fluidic Device, *ACS Sustain. Chem. Eng.*, 2024, **12**, 5533–5543, DOI: 10.1016/j.jclepro.2025.145006.
31 M. Jellicoe, *et al.*, Vortex fluidic induced mass transfer across immiscible phases, *Chem. Sci.*, 2022, **13**, 3375–3385, DOI: 10.1039/D1SC05829K.
32 J. Britton, L. M. Meneghini, C. L. Raston and G. A. Weiss, Accelerating enzymatic catalysis using vortex fluidics, *Angew Chem. Int. Ed. Engl.*, 2016, **55**, 11387–11391, DOI: 10.1002/anie.201604014.
33 T. E. Solheim, F. Salvemini, S. B. Dalziel and C. L. Raston, Neutron imaging and modelling inclined vortex driven thin films, *Sci. Rep.*, 2019, **9**, 2817.
34 T. M. Alharbi, *et al.*, Sub-micron moulding topological mass transport regimes in angled vortex fluidic flow, *Nanoscale Adv.*, 2021, **3**, 3064–3075, DOI: 10.1039/D1NA00195G.
35 C. Chuah, X. Luo, J. Tavakoli, Y. Tang and C. L. Raston, Thin-film flow technology in controlling the organization of materials and their properties, *Aggregate*, 2024, **5**, e433, DOI: 10.1002/agt2.433.

36 J. Britton, K. A. Stubbs, G. A. Weiss and C. L. Raston, Vortex Fluidic Chemical Transformations, *Chem.—Eur. J.*, 2017, **23**, 13270, DOI: **10.1002/chem.201700888**.

37 M. Jellicoe, K. Vimalanathan, J. R. Gascooke, X. Luo and C. L. Raston, High shear spheroidal topological fluid flow induced coating of polystyrene beads with C 60 spicules, *Chem. Commun.*, 2021, **57**, 5638–5641, DOI: **10.1039/D0CC07165J**.

38 X. Luo, *et al.*, Printable Hydrogel Arrays for Portable and High-Throughput Shear-Mediated Assays, *ACS Appl. Mater. Interfaces*, 2023, **15**, 31114–31123, DOI: **10.1021/acsami.3c02353**.

39 E. K. Sitepu, *et al.*, Vortex fluidic mediated direct transesterification of wet microalgae biomass to biodiesel, *Bioresour. Technol.*, 2018, **266**, 488–497, DOI: **10.1016/j.biortech**.

40 X. Cao, *et al.*, Fluidic Mediated Generation of Fatty Acid Ethyl Esters from Vegetable Oils for Applications in Cosmetic Emulsions, *J. Cleaner Prod.*, 2025, **494**, 145006, DOI: **10.1016/j.jclepro.2025.145006**.

41 M. Berrios, M. A. Martín, A. F. Chica and A. Martín, Study of esterification and transesterification in biodiesel production from used frying oils in a closed system, *Chem. Eng. J.*, 2010, **160**, 473–479, DOI: **10.1016/j.cej.2010.03.050**.

42 C. A. Schneider, W. S. Rasband and K. W. Eliceiri, NIH Image to ImageJ: 25 years of image analysis, *Nat. Methods*, 2012, (9), 671–675, DOI: **10.1038/nmeth.2089**.

43 B. Başyiğit, H. Sağlam, İ. Hayoğlu and M. Karaaslan, Spectroscopic (LC-ESI-MS/MS, FT-IR, NMR) and functional characterization of fruit seed oils extracted with green technology: A comparative study with Prunus cerasus and Punica granatum oils, *J. Food Process. Preserv.*, 2021, **45**, e15451, DOI: **10.1111/jfpp.15451**.

44 R. Guzatto, D. Defferrari, Q. B. Reiznautt, Í. R. Cadore and D. Samios, Transesterification double step process modification for ethyl ester biodiesel production from vegetable and waste oils, *Fuel*, 2012, **92**, 197–203, DOI: **10.1016/j.fuel.2011.08.010**.

45 J. Britton and C. Raston, Continuous flow vortex fluidic production of biodiesel, *RSC Adv.*, 2014, **4**, 49850–49854, DOI: **10.1039/C4RA10317C**.

46 V. Mandari and S. K. Devarai, Biodiesel production using homogeneous, heterogeneous, and enzyme catalysts via transesterification and esterification reactions: A critical review, *BioEnergy Res.*, 2022, **15**, 935–961, DOI: **10.1007/s12155-021-10333-w**.

47 A. Negi, S. Nimbkar, R. Thirukumaran, J. Moses and V. Sinija, Impact of thermal and nonthermal process intensification techniques on yield and quality of virgin coconut oil, *Food Chem.*, 2024, **434**, 137415, DOI: **10.1016/j.foodchem.2023.137415**.

48 S. He, *et al.*, Upsized Vortex Fluidic Device Enhancement of Mechanical Properties and the Microstructure of Biomass-Based Biodegradable Films, *ACS Sustain. Chem. Eng.*, 2021, **9**, 14588–14595, DOI: **10.1021/acssuschemeng.1c05534**.

49 R. A. Lodge and B. Bhushan, Wetting properties of human hair by means of dynamic contact angle measurement, *J. Appl. Polym. Sci.*, 2006, **102**, 5255–5265, DOI: **10.1002/app.24774**.

50 J. Gubitosa, V. Rizzi, P. Fini and P. Cosma, Hair Care Cosmetics: From Traditional Shampoo to Solid Clay and Herbal Shampoo, A Review, *Cosmetics*, 2019, **6**, 13, DOI: **10.3390/cosmetics6010013**.

51 A. L. Miranda-Vilela, A. J. Botelho and L. A. Muehlmann, An overview of chemical straightening of human hair: technical aspects, potential risks to hair fibre and health and legal issues, *Int. J. Cosmet. Sci.*, 2014, **36**, 2–11, DOI: **10.1111/ics.12093**.

52 T. Schlake, Determination of hair structure and shape, *Semin. Cell Dev. Biol.*, 2017, **18**, 267–273, DOI: **10.1016/j.semcdb.2007.01.005**.

53 G. S. Luengo, F. Leonforte, A. Greaves, R. G. Rubio and E. Guzman, Physico-chemical challenges on the self-assembly of natural and bio-based ingredients on hair surfaces: towards sustainable haircare formulations, *Green Chem.*, 2023, **25**, 7863–7882, DOI: **10.1039/D3GC02763E**.

54 O. A. Elkady, I. M. Mannaa and M. H. El Bishbishy, Evaluation and formulation of Spirulina platensis proteins for potential applications in hair care products, *Discover Appl. Sci.*, 2024, **6**, 151, DOI: **10.1007/s42452-024-05805-5**.

55 B. Wang, W. Yang, J. McKittrick and M. A. Meyers, Keratin: Structure, mechanical properties, occurrence in biological organisms, and efforts at bioinspiration, *Prog. Mater. Sci.*, 2016, **76**, 229–318, DOI: **10.1016/j.pmatsci.2015.06.001**.

56 C. R. Robbins and C. R. Robbins, Chemical composition of different hair types, *Chemical and Physical Behavior of Human Hair*, 2012, pp. 105–176, DOI: **10.1007/978-3-642-25611-0_2**.

57 M. Hordinsky, S. Chu, A. P. A. Caramori and J. C. Donovan, Hair Physiology and Grooming, *Cosmetic Dermatology: Products and Procedures*, 2022, pp. 299–308, DOI: **10.1002/9781119676881.ch31**.

58 H. K. Bustard and R. W. Smith, Investigation into the scattering of light by human hair, *Appl. Opt.*, 1991, **30**, 3485–3491, DOI: **10.1364/AO.30.003485**.

59 M. F. R. G. Dias, Hair cosmetics: an overview, *Int. J. Trichology*, 2015, **7**, 2, DOI: **10.4103/0974-7753.153450**.

60 D. J. Genders, N. L. Weinberg and C. Zawodzinski, The Direct Electrosynthesis of L-Cysteine Free Base, *Electroorg. Synth.*, 2023, 273–280.

61 Y. Zhang, R. J. Alsop, A. Soomro, F.-C. Yang and M. C. Rheinstädter, Effect of shampoo, conditioner and permanent waving on the molecular structure of human hair, *PeerJ*, 2015, **3**, e1296, DOI: **10.7717/peerj.1296**.

62 J. M. Marsh, *et al.*, Gel network shampoo formulation and hair health benefits, *Int. J. Cosmet. Sci.*, 2017, **39**, 543–549, DOI: **10.1111/ics.12409**.

63 T. Takahashi and S. Yoshida, A highly resistant structure between cuticle and cortex of human hair, *Int. J. Cosmet. Sci.*, 2017, **39**, 327–336, DOI: **10.1111/ics.12380**.

64 R. A. Boulos, *et al.*, Unravelling the structure and function of human hair, *Green Chem.*, 2013, **15**, 1268–1273, DOI: **10.1039/c3gc37027e**.

65 H. Zhang, F. Carrillo-Navarrete, M. Lopez-Mesas and C. Palet, Use of Chemically Treated Human Hair Wastes for the Removal of Heavy Metal Ions from Water, *Water*, 2020, **12**, 1263, DOI: **10.3390/w12051263**.

66 L. Mester, A. A. Govyadinov, S. Chen, M. Goikoetxea and R. Hillenbrand, Subsurface chemical nanoidentification by nano-FTIR spectroscopy, *Nat. Commun.*, 2020, **11**, 3359, DOI: **10.1038/s41467-020-17034-6**.

67 H. Gao, B. Ji, I. L. Jäger, E. Arzt and P. Fratzl, Materials become insensitive to flaws at nanoscale: lessons from nature, *Proc. Natl. Acad. Sci. U. S. A.*, 2003, **100**, 5597–5600, DOI: **10.1073/pnas.0631609100**.

68 E. Demir and N. Acaralı, Comparison on Quality Performance of Human Hair Types with Herbal Oils (Grape Seed/Safflower Seed/Rosehip) by Analysis Techniques, *ACS Omega*, 2023, **8**, 8293–8302, DOI: **10.1021/acsomega.2c06550**.